Available online at www.sciencedirect.com
ScienceDirect
Polymer 48 (2007) 4867–4873
polymer
www.elsevier.com/locate/polymer

Fracture behavior of nanocomposites based on poly (ethylene-*co*-methacrylic acid) ionomers

Youngjae Yoo, Rhutesh K. Shah[1], D.R. Paul*

Department of Chemical Engineering and Texas Materials Institute, The University of Texas at Austin, Austin, TX 78712, United States

Received 23 March 2007; received in revised form 4 June 2007; accepted 5 June 2007
Available online 9 June 2007

Abstract

The fracture behavior of nanocomposites formed from an organoclay, based on montmorillonite (MMT), and a poly(ethylene-*co*-methacrylic acid) ionomer prepared by melt compounding was investigated using an instrumented impact test. The data were analyzed using the essential work of fracture (EWF) methodology. Transmission electron microscopy revealed that the clay platelets were well-exfoliated in this matrix. The fracture energy of these nanocomposites increased with organoclay addition at low concentrations but decreased with further increase in organoclay concentration with a maximum between 2 and 3 wt% MMT. The initial increase in fracture energy is a result of the higher forces during loading caused by the increase in modulus and yield stress upon addition of clay; however, the fracture energy eventually decreases with further addition of clay owing to the continuous decrease in ductility or deflection during testing. The EWF of fracture analysis showed that the energy per unit area of crack surface formed exhibits a maximum at 2–3 wt% MMT while the energy dissipated per unit volume in the surrounding process zone decreases monotonically for all clay loadings with a transition from ductile to brittle behavior occurring at 7–8 wt% MMT.

Keywords: Nanocomposite; Ionomer; Fracture

1. Introduction

Since Toyota commercialized polyamide 6/clay nanocomposites for heat-resistant automotive timing belt covers, polymer/clay nanocomposites have attracted much interest from academic and industrial researchers [1–3]. The most commonly used clay is montmorillonite (MMT) whose sodium ions are usually ion-exchanged with an organic ammonium-based surfactant to make an organoclay that is more compatible with polymers. The 1 nm thick clay platelets have a high aspect ratio which allows well-exfoliated polymer/organoclay nanocomposites to exhibit greater reinforcement at a lower volume fraction of filler than conventional composites [4–6]. Numerous studies have demonstrated significant enhancements in stiffness and strength [7,8], flame retardancy [9,10], gas barrier properties [11,12], thermal stability [13] and ionic conductivity [14,15]. Numerous polymer matrices have been considered including polyamide 6 [4,16], polypropylene [17–20], polycarbonate [21], polystyrene [22,23], and others.

The significant enhancement in modulus and strength observed for polymer/organoclay nanocomposites is reasonably well understood. However, the one property that mostly decreases relative to that of the matrix polymer is toughness; indeed, most polymers show decreased toughness when organoclays are added [4,24–26]. Our previous report, however, showed increased toughness at low clay loading for nanocomposites formed from poly(ethylene-*co*-methacrylic acid) ionomers as evaluated by the Izod impact test; at higher clay loading the impact strength decreased [27]. This unusual result is quite different from many reports about mechanical properties of polymer nanocomposites [4,21,24–29]; however, a few other studies have also reported increased toughness

* Corresponding author. Tel.: +1 512 471 5392; fax: +1 512 471 0542.
E-mail address: drp@che.utexas.edu (D.R. Paul).
[1] Present address: School of Engineering and Applied Sciences (SEAS), Harvard University, Cambridge, MA 02138, USA.

0032-3861/$ - see front matter © 2007 Elsevier Ltd. All rights reserved.
doi:10.1016/j.polymer.2007.06.007

caused by adding clay [30,31]. The aim of this paper is to investigate the fracture behavior of such nanocomposites in more detail to understand the toughness changes more clearly using an instrumented impact test and analysis of the data using the essential work of fracture (EWF) methodology.

2. Background

The Izod and Charpy impact tests are the most widely used methods to measure the fracture behavior of polymeric materials because the measurements are simple and convenient. However, these tests only give the energy required to fracture a specimen of a fixed geometry which does not lead to deep understanding of the toughness of the polymeric material. Moreover, in the case of ductile materials, samples frequently show only partial breaks [28]. Instrumented impact testing of samples having a sharp notch with a range of ligament lengths combined by analysis of the data using the essential work of fracture, EWF, method can be a more effective way to understand the fractures behavior of nanocomposites like those made from poly(ethylene-*co*-methacrylic acid) ionomers mentioned above. Since the EWF method was first developed by Broberg [32], it has been successfully applied to polymeric materials to quantify the effects contributing to the energy involved in fracturing a relatively ductile material [33–35]. In this analysis, two separate zones are visualized: (a) an inner fracture process zone in which the initiation and propagation of the crack occur and (b) a surrounding outer zone in which energy is absorbed by plastic deformation during the crack extension [36]. Mai and Cotterell [37,38] have developed a methodology based on Broberg's unified theory of fracture [39,40] for evaluating the fracture behavior of polymeric materials. According to their reports, the total work of fracture during crack growth, W_f or U (generally referenced as the total fracture energy), can be divided into the essential work or energy associated with the inner fracture process zone, W_e, and the non-essential plastic work or the energy associated with the plastic deformation in the non-EWF in the outer plastic zone, W_p,

$$W_f = W_e + W_p \tag{1}$$

They proposed the following equation based on the assumptions that W_e is proportional to the fracture area and W_p is proportional to the volume of the plastic zone

$$w_f = \frac{W_f}{A} = w_e + \beta w_p \ell \tag{2}$$

where, w_f is the total specific work of fracture, w_e is the specific essential work of fracture, w_p is the specific non-essential plastic work of fracture, β is a shape factor, A is the fracture surface area, and ℓ is the ligament length. From this relationship, w_f is dependent on specimen geometry and increases linearly with increasing ℓ with a slope of βw_p and an intercept of w_e. The model assumes that the ligament must be fully yielded prior to crack initiation and, thus, has certain limitations on the ligament length.

In what follows, we use an instrumented impact test where a single-edge notched specimen is loaded in three-point bending; the recorded load–displacement curve can be integrated to give the fracture energy. Experimental conditions in this study are similar to those used by Vu-Khanh (thick specimens and high speed loading). In this case, the yielding and ligament length size criteria of the EWF method proposed by Mai and coworkers may not always be satisfied in the high speed bending configuration used in this study; however, the results may still be evaluated using the EWF methodology. The slope and intercept from plots of w_f versus ligament length may not necessarily have the same physical meanings that have been assigned to βw_p and w_e. Thus, a different nomenclature is employed here as in previous papers [36,41–44].

$$\frac{U}{A} = u_0 + u_d \ell \tag{3}$$

The term u_0 represents a limiting specific fracture energy while u_d is the dissipative energy density. Under appropriate conditions, $u_0 = w_e$ and $u_d = \beta w_p$. These parameters should be considered phenomenological in nature and may not always be material parameters. The current work is intended to provide a deeper understanding of the fracture toughness of the nanocomposites than provided by simple Izod testing.

3. Experimental

3.1. Materials and composite preparation

A commercial grade ionomer, Surlyn® 8945, was purchased from duPont. This ionomer is a copolymer of ethylene and methacrylic acid where some of the acid groups have been neutralized to form the sodium salt. The organoclay used in this study, Cloisite® 20A, was prepared by an ion exchange reaction between sodium montmorillonite (Na-MMT) and an amine surfactant. Cloisite® 20A is a commercial product of Southern Clay Products, Inc. and was used as-received. Table 1 provides details about the materials used in this study.

Prior to melt processing, Surlyn® 8945 was dried for a minimum of 48 h in a vacuum oven at 65 °C while organoclay was used as-received. Blending was accomplished in a Haake co-rotating, intermeshing twin screw extruder (diameter = 30 mm, $L/D = 10$) using a barrel temperature of 200 °C, a screw speed of 280 rpm, and a feed rate of 1200 g/h. All materials were added simultaneously into the hopper of the extruder to obtain a nanocomposite of the desired composition. After extrusion, the materials were dried again in a vacuum oven and molded into 6.35 mm thick bars for impact testing via an Arburg Allrounder 305-210-700 injection molding machine using a barrel temperature of 220 °C, mold temperature of 45 °C, injection pressure of 70 bar and a holding pressure of 40 bar.

Table 1
Materials used in this study

Material	Commercial designation	Specifications	Supplier
Sodium ionomer of poly(ethylene-*co*-methacrylic acid)	Surlyn 8945	MI = 4.5 g/10 min; specific gravity = 0.96; methacrylic acid content = 15.2 wt%; sodium content = 1.99 wt%; neutralization = ~40%	E.I. du Pont de Nemours and Company
Organoclay:[a] dimethyl bis(hydrogenated-tallow) ammonium montmorillonite	Cloisite 20A	Organic loading = 95 mequiv/100 g clay; organic content = 39.6 wt%; d_{001} spacing[b] = 25.5 Å	Southern Clay Products

[a] The selected organoclay is designated as $M_2(HT)_2$ in this study, where M = methyl and HT = hydrogenated-tallow. Tallow is a natural product composed predominantly (63%) of saturated and unsaturated C_{18} chains. HT is the saturated form yet still contains a small fraction of double bonds.
[b] The basal spacing corresponds to the characteristic Bragg reflection peak d_{001} obtained from a powder WAXS scan of the organoclay.

3.2. Dynatup fracture test and morphology characterization

An instrumented impact test (Dynatup model 8200 drop tower) with an attached computer for data acquisition was used to load a single-edge notched specimen in three-point bending. The recorded load–displacement curve can be integrated to give the fracture energy. The sample dimensions were 56 mm in length, 12.7 mm in width and 6.35 mm in thickness. Each test was performed with a tup mass of 14 kg (81 J capacity at the impact velocity) falling at approximately 3.4 m/s. The injection molded specimens were cut into 5.6 cm

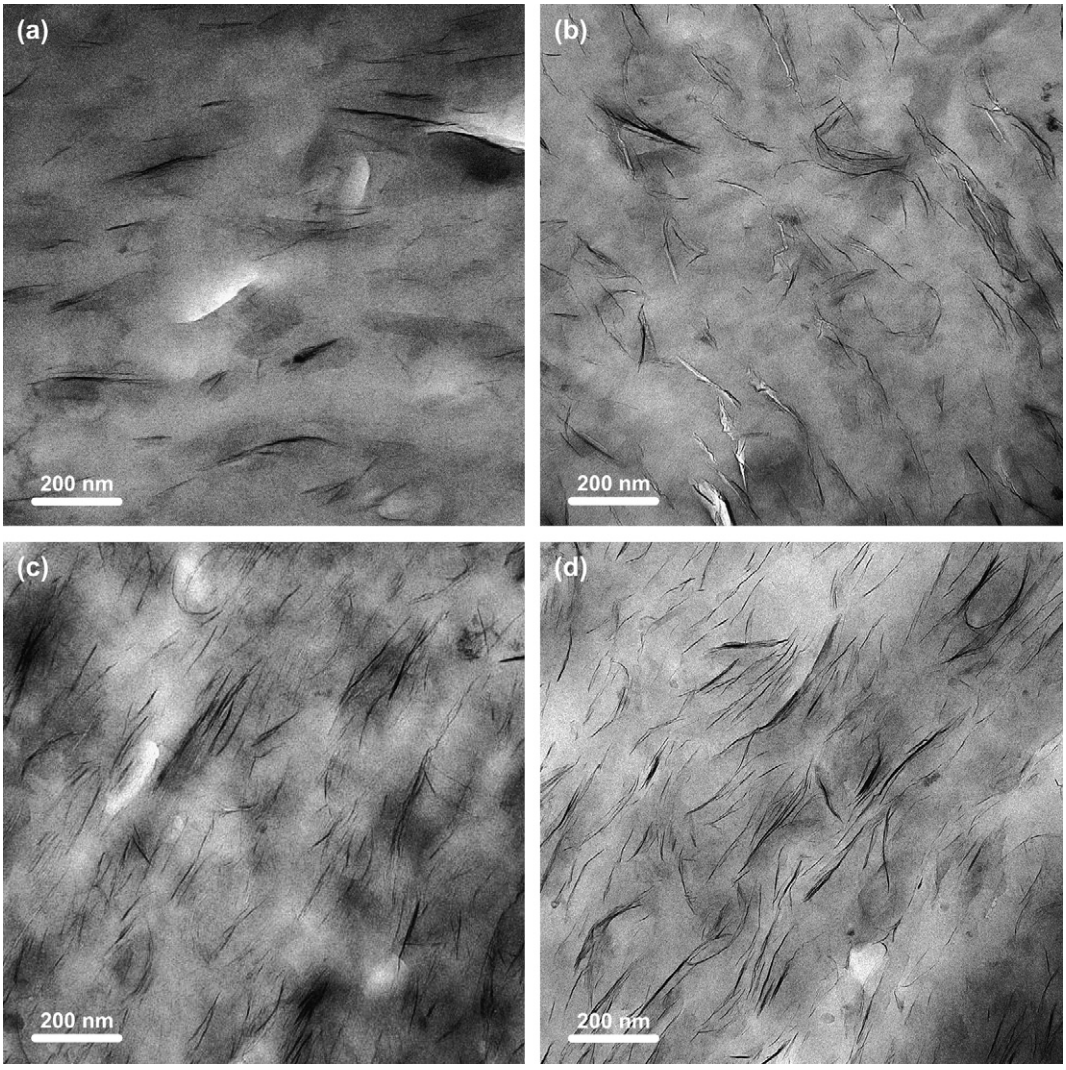

Fig. 1. TEM photomicrographs of nanocomposites based on poly(ethylene-*co*-methacrylic acid) ionomer showing clay particle morphology for MMT contents of 2.5 wt% (a), 4.5 wt% (b), 5.5 wt% (c), and 7.5 wt% (d). Images were taken from the core and viewed parallel to the transverse direction, TD, of injection molded bars.

in length and pre-notched at the center with a band saw. In each test, 24 samples were used with six different ligament lengths (2, 4, 5, 6, 8, 10 mm); four samples (two far end and two gate end specimens) were used for each ligament length. A sharp notch was created by tapping a fresh regular duty razor blade (0.23 mm thick) into the pre-notch. Rubber pads and rubber bands were used to cover the tup to reduce mechanical damping and to secure the sample ends to the testing frame; the rubber pad was made from six layers of (large size) Safeskin® latex rubber gloves. The fracture energy was evaluated from a numerical integration of the load–displacement data. More details about the Dynatup fracture test and the sample geometry are available elsewhere [33,34,36,41–45].

Samples for morphology analysis were taken from the core portion of an injection molded bar. Ultra-thin sections of approximately 50 nm in thickness were cryogenically cut with a diamond knife and cooled using liquid nitrogen at a temperature of −40 °C using a Reichert-Jung Ultracut E microtome. These sections were taken from the plane defined by the flow direction (FD) and the transverse direction (TD) of the molded bar as explained elsewhere [13]. Sections were collected using 300 mesh grids and dried using filter paper. The morphology was examined using JEOL 2010F transmission electron microscopy (TEM) equipped with a field emission gun at an accelerating voltage of 120 kV.

4. Results and discussion

4.1. Morphology analysis by TEM

TEM observations were made to verify if exfoliation of MMT into the matrix material was achieved and to qualitatively assess the degree of exfoliation of the MMT platelets. Fig. 1 shows a series of TEM micrographs for the ionomer nanocomposites as a function of MMT content. Over the range of MMT concentrations examined, the nanocomposites exhibit excellent, uniform dispersion of MMT with no visible large MMT tactoids. These results are consistent with the wide angle X-ray diffraction (WAXD) and TEM analyses shown in a previous paper from our group [27].

4.2. Force versus displacement curves

Because of the high velocity (approximately 3.4 m/s) at which the tup strikes the sample in the Dynatup test, significant vibrations occur during the three-point bending resulting in noisy force versus deflection curves. In order to provide a more reasonable picture of the force–deflection process, these curves were smoothed by fitting each peak to a Gaussian–Lorentzian shape and subtracting the oscillations. The smoothing process had negligible effect on the area under the load–displacement curve. Fig. 2(a) and (b) shows representative examples of the raw and smoothed data from tests made with ligament lengths of 4 mm and 8 mm for samples containing 0 and 7.5 wt% MMT. Fig. 3 shows two typical load–displacement curves for nanocomposites of poly(ethylene-*co*-methacrylic acid) ionomer containing 0–10 wt%

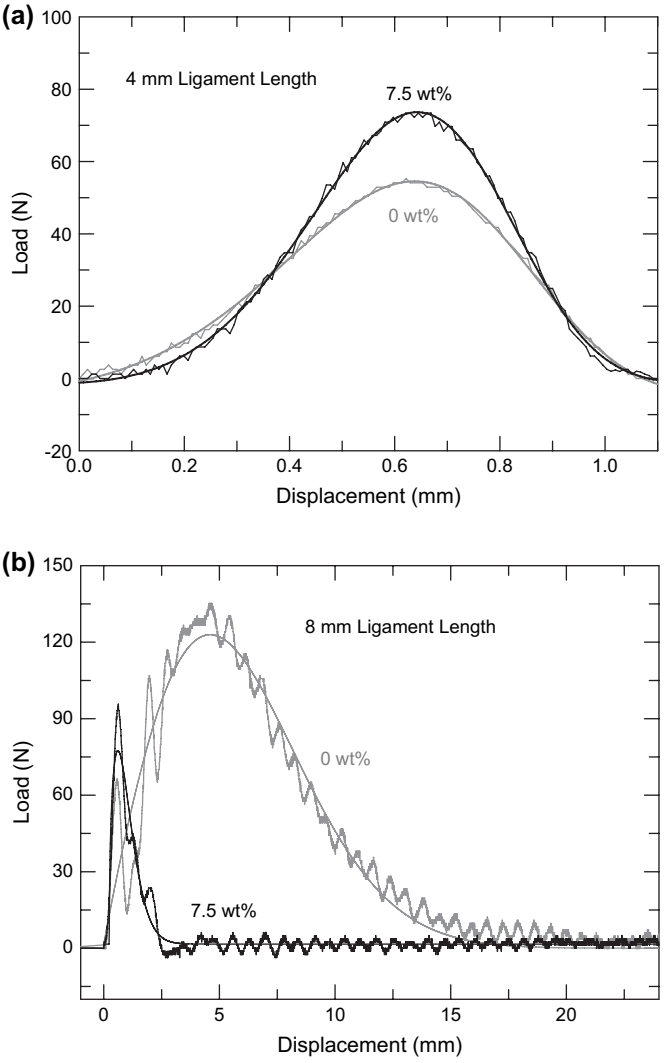

Fig. 2. Illustration of the smoothing procedure for load–displacement data of nanocomposites prepared from poly(ethylene-*co*-methacrylic acid) ionomer.

MMT. Correction for drift in the baseline was made on all measurements. Under the conditions imposed here, nanocomposite test specimens with short ligament lengths (4 mm) show quite brittle behavior while samples with larger ligament lengths (8 mm) may show either brittle or ductile behavior. As seen in Fig. 3(a), ionomer specimens with short ligaments reach a load of approximately 55 N before sharply dropping off in the characteristic manner of brittle failure. As the content of MMT increases, the maximum load recorded also increases. Nanocomposites with 10 wt% MMT exhibit brittle fracture; however, in this case, fracture occurs at much higher load, approximately, 78 N. Nanocomposite test specimens with large ligament lengths (8 mm) show quite different behavior as seen in Fig. 3(b). The specimen of the neat ionomer and of nanocomposites with low clay loading (1.0–3.5 wt%) exhibits larger maximum loads and displacements relative to the specimens with small ligament lengths. A maximum load of 180 N was measured for the nanocomposite containing 3.5 wt% MMT. For the larger ligament lengths, the specimens undergo yielding and the load trails off gradually rather than

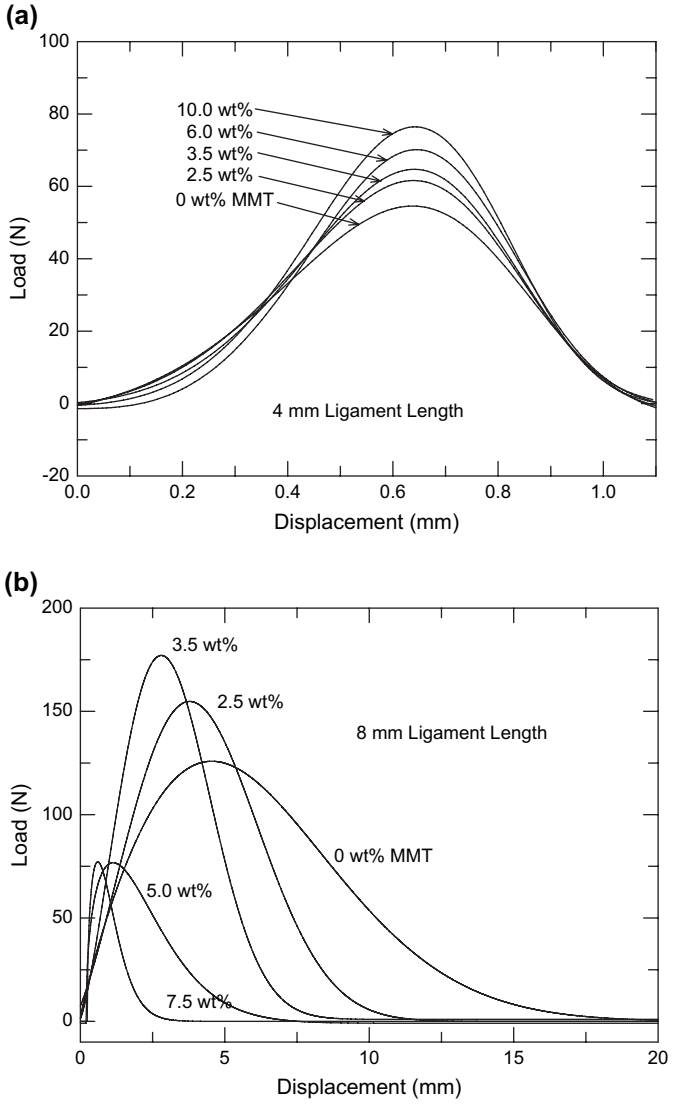

Fig. 3. Load–displacement data of nanocomposites from poly(ethylene-*co*-methacrylic acid) ionomer containing 0–10 wt% MMT.

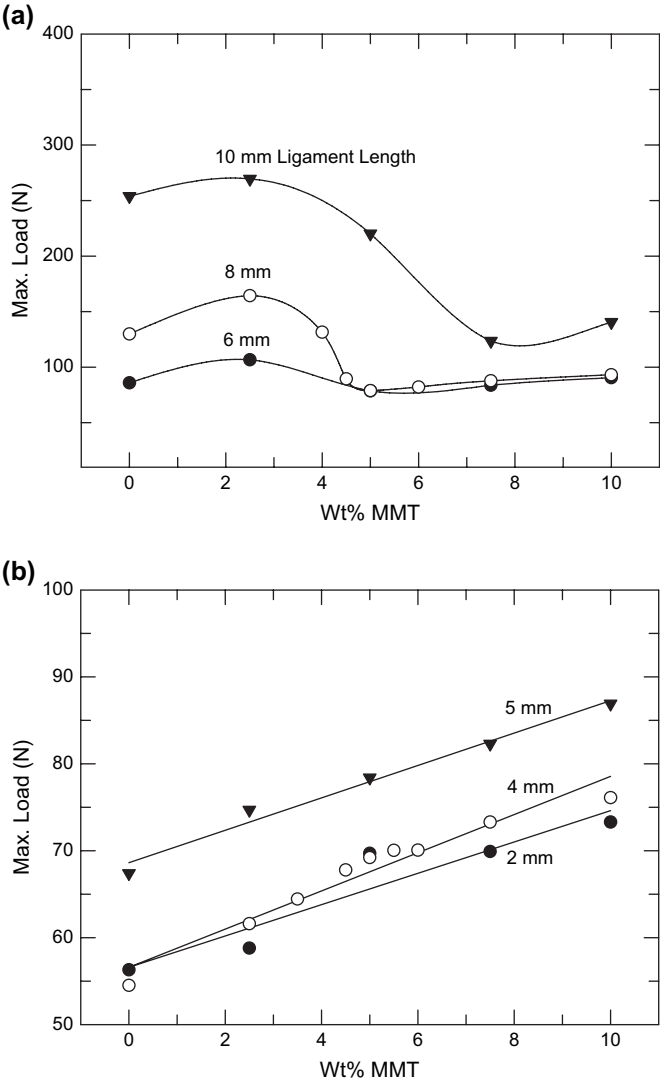

Fig. 4. Maximum load absorbed in Dynatup force–displacement measurements versus MMT loading at different ligament lengths for nanocomposites based on poly(ethylene-*co*-methacrylic acid) ionomer.

dropping sharply as shown in Fig. 3(a) for the shorter ligament. These extended tails after yielding are typical of ductile failure. When 4.0 wt% or more of MMT is added, the maximum load gradually decreases and the ductile behavior gives way to brittle failure. Fig. 4 shows the maximum load versus wt% MMT for nanocomposite test specimens with six different ligament lengths. For a clear analysis of the relationship among the maximum load, wt% MMT and ligament length, the plots for the larger (6, 8, 10 mm) and smaller (2, 4, 5 mm) ligament lengths are shown using different scales. For larger ligament lengths, the maximum load increases with MMT addition for low concentrations, but decreases with further increases in MMT concentration. Also, the highest maximum loads were observed for nanocomposite samples containing 2.5 wt% MMT over the whole range of larger ligament lengths. For shorter ligament lengths, however, the maximum load is much smaller and increases linearly with the concentration of MMT as seen in Fig. 4(b).

4.3. Essential work of fracture analysis

Because of the disadvantages and limitations of the Izod and Charpy impact tests, for this study Dynatup impact tests on samples having a sharp notch with various ligament lengths combined by analysis of the data using the EWF method were chosen as a more effective way to understand the fracture behavior of these nanocomposites. Fig. 5 shows the total fracture energy per unit area, U/A, versus ligament length for nanocomposites containing 0–10 wt% MMT. Up to 2.5 wt% MMT, the materials show ductile fracture and U/A increases linearly with the ligament length; the values of U/A increase with clay content up to about 2.5 wt% MMT. For 5.0 wt% MMT and higher, the nanocomposites show brittle behavior and U/A becomes more or less independent of ligament length and decreases in absolute value with increasing MMT concentration. Fig. 6 shows the total fracture energy per unit area, U/A, for two ligament lengths, 4 mm and 8 mm, as a function

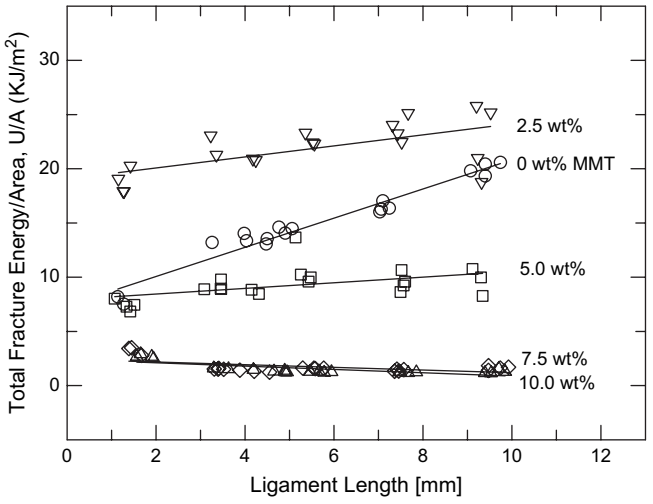

Fig. 5. Total fracture energy per unit area, U/A, versus ligament length for nanocomposites of poly(ethylene-*co*-methacrylic acid) ionomer containing from 0 to 10 wt% MMT.

of MMT content. Irrespective of ligament length, the specific fracture energy obtained by the Dynatup impact test increases with MMT at low concentrations, but then decreases gradually with further increase in MMT concentration. The maximum specific fracture energy achieved at low MMT contents is greater for large ligament lengths than for small ligament lengths. These trends are in a good agreement with the Izod results in our previous report on similar materials [27]. As mentioned earlier, this initial increase in fracture energy with addition of clay is somewhat unexpected based on prior literature which generally shows a monotonic decrease in ductility or fracture toughness when organoclays are added [4,21,24–29]. The Dynatup data reveal that the increased fracture energy at low MMT concentrations observed here reflects the increased stiffness and yield strength that overshadows the loss in ductility resulting in a larger area under the force–deflection curves. Fig. 3 shows that the maximum load

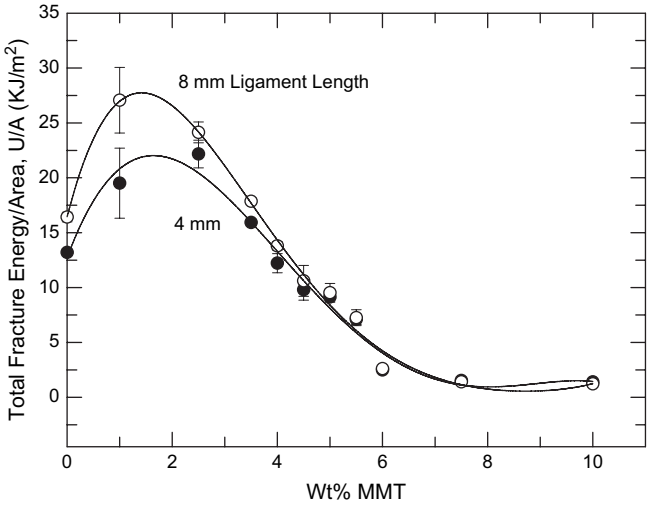

Fig. 6. Effect of MMT content on the total fracture energy per unit area, U/A, for nanocomposites based on poly(ethylene-*co*-methacrylic acid) ionomer.

experienced by the nanocomposite samples increases with MMT content up to about 3.5 wt%. However, the loss in ductility or amount of deflection at higher MMT concentrations is much greater and the nanocomposites begin to show brittle behavior and the maximum load experienced by the samples is decreased.

Fig. 7 shows the limiting specific fracture energy, u_0, and the dissipative energy density, u_d, as defined by Eq. (3) obtained from plots of U/A versus ligament length as a function of clay content. Clearly, u_0 follows very similar behavior as the total fracture energy shown in Fig. 6; i.e., there is a maximum value in u_0 between 2 and 3 wt% MMT. This means the energy absorbed per unit area in the region surrounding the fracture surface increases at low MMT concentration and then decreases at higher MMT concentration. As shown in Fig. 7(b), the dissipative energy density, u_d, decreases continuously with MMT concentration over the whole range of loading. The term, u_d, is associated with energy absorbing

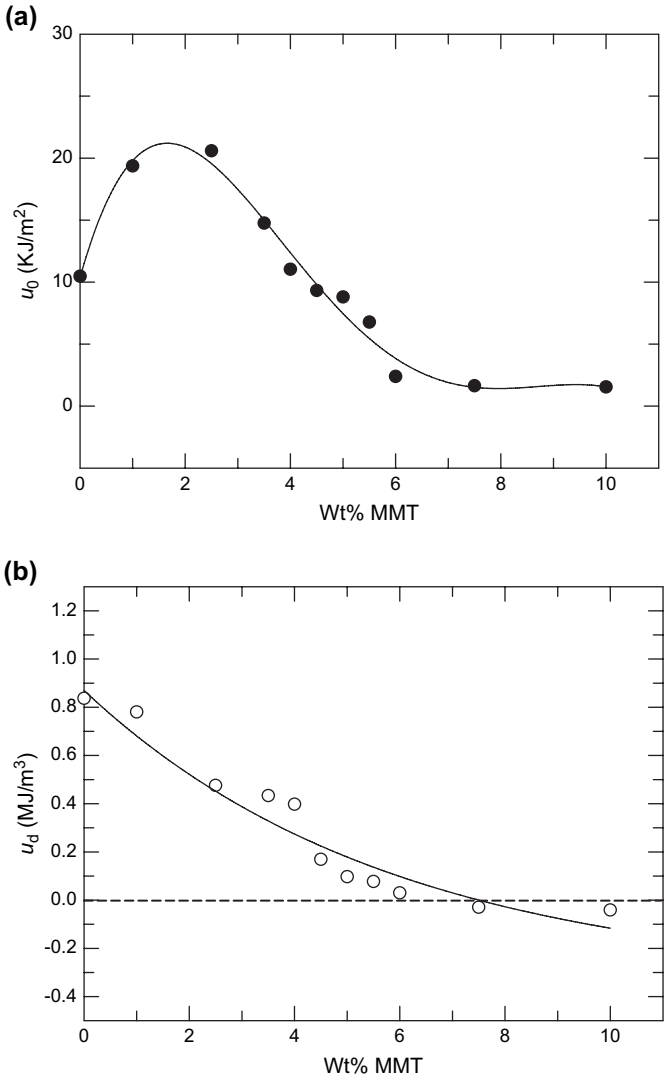

Fig. 7. Effect of MMT content on the limiting specific fracture energy, u_0 (a) and the dissipative energy density, u_d (b), for nanocomposites based on poly(ethylene-*co*-methacrylic acid) ionomer.

processes, e.g., shear yielding, in the process zone away from the fracture surface [45]. Evidently, the addition of MMT to the poly(ethylene-*co*-methacrylic acid) ionomer reduces the large-scale plastic deformation away from the fracture surface because of the constraints imposed upon the matrix by the MMT particles. A transition from a positive slope to a negative slope of U/A versus ligament length was observed between 7 and 8 wt% of MMT and marks a ductile to brittle transition at this concentration of MMT.

5. Conclusions

Nanocomposites from poly(ethylene-*co*-methacrylic acid) ionomers and commercial organoclay were prepared by melt blending; the exfoliated structure was assessed qualitatively by TEM analysis. The toughness or fracture energy of these materials increased with organoclay addition at low concentrations but decreased on further increase in organoclay concentration. The optimum concentration to achieve the maximum total fracture energy lies between 2 and 3 wt% MMT. Two opposing effects give rise to this maximum in energy to fracture or area under the force–deflection curve. Addition of clay increases the stiffness and the yield strength but reduces the amount of deformation possible. At low clay contents the higher loads cause an increased area under the curve but eventually the loss of ductility becomes the dominant factor and the area under the curve decreases. An essential work of fracture, EWF, analysis shows that the energy per unit area of crack surface formed, u_0, versus clay content shows a maximum at 2–3 wt% MMT similar to the area under the force versus deflection curves for any fixed ligament length. On the other hand, the energy dissipated per unit volume, u_d, in the outer zone surrounding the crack surface by ductile processes like shear yielding, continuously decreases with added clay. The value of u_d goes from positive to negative at 7–8 wt% MMT defining a brittle to ductile transition concentration.

Acknowledgements

The authors sincerely thank P. J. Yoon and D. L. Hunter of Southern Clay Products, Inc. for providing organoclay materials, and many helpful discussions.

References

[1] Usuki A, Kojima Y, Kawasumi M, Okada A, Fukushima Y, Kurauchi T, et al. J Mater Res 1993;8(5):1185–9.
[2] Usuki A, Kojima Y, Kawasumi M, Okada A, Fukushima Y, Kurauchi T, et al. J Mater Res 1993;8(5):1179–84.
[3] Kojima Y, Usuki A, Kawasumi M, Okada A, Kurauchi T, Kamigaito O. J Polym Sci Part A Polym Chem 1993;31(4):983–6.
[4] Fornes TD, Yoon PJ, Keskkula H, Paul DR. Polymer 2001;42(25):9929–40.
[5] Yoo Y, Choi K-Y, Lee JH. Macromol Chem Phys 2004;205(14):1863–8.
[6] Yoo Y, Kim S-S, Won JC, Choi K-Y, Lee JH. Polym Bull 2004;52(5):373–80.
[7] Liu L, Qi Z, Zhu X. J Appl Polym Sci 1999;71(7):1133–8.
[8] Wang Z, Pinnavaia TJ. Chem Mater 1998;10(12):3769–71.
[9] Hu Y, Wang S, Ling Z, Zhuang Y, Chen Z, Fan W. Macromol Mater Eng 2003;288(3):272–6.
[10] Schmidt D, Shah D, Giannelis EP. Curr Opin Solid State Mater Sci 2002;6(3):205–12.
[11] Messersmith PB, Giannelis EP. J Polym Sci Part A Polym Chem 1995;33(7):1047–57.
[12] Yano K, Usuki A, Okada A, Kurauchi T, Kamigaito O. J Polym Sci Part A Polym Chem 1993;31(10):2493–8.
[13] Yoon PJ, Fornes TD, Paul DR. Polymer 2002;43(25):6727–41.
[14] Chen W, Xu Q, Yuan RZ. Mater Sci Eng B 2000;77(1):15–8.
[15] Chen W, Xu Q, Yuan RZ. Compos Sci Technol 2001;61(7):935–9.
[16] Fornes TD, Yoon PJ, Hunter DL, Keskkula H, Paul DR. Polymer 2002;43(22):5915–33.
[17] Kim DH, Park JU, Ahn KH, Lee SJ. Macromol Rapid Commun 2003;24(5-6):388–91.
[18] Xu W, Liang G, Wang W, Tang S, He P, Pan W-P. J Appl Polym Sci 2003;88(14):3225–31.
[19] Ton-That M-T, Perrin-Sarazin F, Cole KC, Bureau MN, Denault J. Polym Eng Sci 2004;44(7):1212–9.
[20] Kim DH, Cho KS, Mitsumata T, Ahn KH, Lee SJ. Polymer 2006;47(16):5938–45.
[21] Yoon PJ, Hunter DL, Paul DR. Polymer 2003;44(18):5323–39.
[22] Hasegawa N, Okamoto H, Kawasumi M, Usuki A. J Appl Polym Sci 1999;74(14):3359–64.
[23] Stretz HA, Paul DR. Polymer 2006;47(26):8527–35.
[24] Kelnar I, Kotek J, Kaprálková L, Munteanu BS. J Appl Polym Sci 2005;96(2):288–93.
[25] Tanniru M, Yuan Q, Misra RDK. Polymer 2006;47(6):2133–46.
[26] Jimenez G, Ogata N, Kawai H, Ogihara T. J Appl Polym Sci 1997;64(11):2211–20.
[27] Shah RK, Hunter DL, Paul DR. Polymer 2005;46(8):2646–62.
[28] Bao SP, Tjong SC. Compos Part A Appl Sci Manufact 2007;38(2):378–87.
[29] Stretz HA, Paul DR, Cassidy PE. Polymer 2005;46(11):3818–30.
[30] Chen L, Wong S-C, Liu T, Lu X, He C. J Polym Sci Part B Polym Phys 2004;42(14):2759–68.
[31] Wang K, Chen L, Wu J, Toh ML, He C, Yee AF. Macromolecules 2005;38(3):788–800.
[32] Broberg KB. Int J Fract 1968;4(1):11–9.
[33] Kayano Y, Keskkula H, Paul DR. Polymer 1998;39(4):821–34.
[34] Kudva RA, Keskkula H, Paul DR. Polymer 1999;41(1):335–49.
[35] Vu-Khanh T. Polymer 1988;29(11):1979–84.
[36] Pressly TG, Keskkula H, Paul DR. Polymer 2001;42(7):3043–55.
[37] Mai YW, Cotterell B. Eng Fract Mech 1985;21(1):123–8.
[38] Mai YW, Cotterell B. Int J Fract 1986;32(2):105–25.
[39] Broberg KB. J Mech Phys Solids 1971;19(6):407–17.
[40] Broberg KB. J Mech Phys Solids 1975;23(3):215–37.
[41] Hale W, Keskkula H, Paul DR. Polymer 1999;40(12):3353–65.
[42] Laura DM, Keskkula H, Barlow JW, Paul DR. Polymer 2001;42(14):6161–72.
[43] Okada O, Keskkula H, Paul DR. Polymer 2000;41(22):8061–74.
[44] Huang JJ, Paul DR. Polymer 2006;47(10):3505–19.
[45] Laura DM, Keskkula H, Barlow JW, Paul DR. Polymer 2003;44(11):3347–61.